Ann. Occup. Hyg.

doi:10.1093/annhyg/met007

Functionality Based Detection of Airborne Engineered Nanoparticles in Quasi Real Time: A New Type of Detector and a New Metric

NICOLE NEUBAUER*, MARTIN SEIPENBUSCH and GERHARD KASPER

Institut für Mechanische Verfahrenstechnik und Mechanik, Karlsruhe Institute of Technology (KIT), Straße am Forum 8, 76131 Karlsruhe, Germany

Received 16 November 2012; in final form 21 January 2013

A new type of detector which we call the Catalytic Activity Aerosol Monitor (CAAM) was investigated towards its capability to detect traces of commonly used industrial catalysts in ambient air in quasi real time. Its metric is defined as the catalytic activity concentration (CAC) expressed per volume of sampled workplace air. We thus propose a new metric which expresses the presence of nanoparticles in terms of their functionality - in this case a functionality of potential relevance for damaging effects - rather than their number, surface, or mass concentration in workplace air. The CAAM samples a few micrograms of known or anticipated airborne catalyst material onto a filter first and then initiates a chemical reaction which is specific to that catalyst. The concentration of specific gases is recorded using an IR sensor, thereby giving the desired catalytic activity. Due to a miniaturization effort, the laboratory prototype is compact and portable. Sensitivity and linearity of the CAAM response were investigated with catalytically active palladium and nickel nano-aerosols of known mass concentration and precisely adjustable primary particle size in the range of 3–30 nm. With the miniature IR sensor, the smallest detectable particle mass was found to be in the range of a few micrograms, giving estimated sampling times on the order of minutes for workplace aerosol concentrations typically reported in the literature. Tests were also performed in the presence of inert background aerosols of SiO_2, TiO_2, and Al_2O_3. It was found that the active material is detectable via its catalytic activity even when the particles are attached to a non-active background aerosol.

Keywords: background distinction; catalytic activity concentration; engineered nanoparticles; functionality based detection; quasi real time

INTRODUCTION

The potential for exposure of workers to engineered nanoparticles has increased significantly in recent years due to a rapidly rising production and use of such materials. The level of exposure to such materials is expected to be higher in workplaces than in other environments (Bergamaschi, 2009) and may occur during the production process, as well as handling and processing of the manufactured particles (Methner et al., 2009; Tsai et al., 2009; Brouwer, 2010). A variety of methods for the detection and monitoring of nanoparticle exposure in the workplace is already in existence and broadly discussed in the literature (Baron and Willeke, 2001; Hester and Harrison, 2007; Maynard and Aitken, 2007; Kuhlbusch et al., 2011). Devices are available for both online and offline analyses, providing concentration information according to different metrics such as mass, surface area or number, either size resolved or as sum total over a specific size range. One difficulty common to most of these techniques is their inherent inability to distinguish between target nanoparticles and background particles in a given size range (Kuhlbusch et al., 2009; Murashov

*Author to whom correspondence should be addressed.
Tel: +0049-721-6084-6573; fax: +0049-721-6084-6563:
e-mail: nicole.neubauer@kit.edu

et al., 2009; Savolainen et al., 2010b) except by time-consuming and expensive measurement campaigns (Brouwer et al., 2009; Kuhlbusch et al., 2011). Furthermore, such techniques do not account for any shift in particle size due to coagulation or other aerosol dynamic mechanisms during the time the aerosol travels between source and human receptor (Seipenbusch et al., 2008). Very small particles have an especially strong tendency to attach themselves to pre-existing background particles (typically in the size range of about 0.1–1 μm). Attachment causes them to 'disappear' from their original size class as measured by the types of instruments mentioned above. Therefore, most studies resort to additional chemical or morphological analyses obtained by expensive offline techniques such as optical and mass spectrometry (Savolainen et al., 2010a; Kuhlbusch et al., 2011) or electron microscopy (Peters et al., 2008). In summary, the rapid and cost-effective discrimination of the target nanoparticles from the background aerosol remains an unresolved issue in the workplace and elsewhere.

Catalytically active particles represent an important class of engineered nanoparticles. Earlier studies have shown in principle that the catalytic activity of airborne metals or metal oxides can be measured with high sensitivity (Neubauer et al., 2011). Based on this concept, we have developed a compact and portable laboratory prototype which we call the Catalytic Activity Aerosol Monitor (CAAM). The CAAM detection principle is based on sampling a defined volume of aerosol during a short period of time (ideally a few minutes, depending on the mass concentration of the aerosol) and then immediately initiating a catalyzed chemical reaction which is specific to the type of nanoparticle material anticipated in the workplace air. The concentrations of specific gases are measured by an integrated IR sensor, hereby providing a measure for the catalytic activity of the particles which can be translated into a catalytic activity concentration (CAC), i.e. an activity per volume of sampled air. Clearly, the CAAM is not intended as an environmental monitor to look for arbitrary types of particle species because it requires *a priori* knowledge of the type of material, which should, however, be available in most workplaces.

In the current paper, this new type of detector is investigated with respect to its sensitivity for two prominent industrial catalysts (palladium and nickel), as well as its capability of discriminating these active nanoparticles against inert background aerosols (SiO_2, TiO_2, Al_2O_3). Required CAAM sampling times for palladium and nickel were estimated on the basis of measured lower mass detection limits and assuming concentrations for such materials typically reported in the literature for workplace air. The aerosols were generated continuously via established laboratory techniques and with adjustable mass concentrations and primary particle sizes. The influence of the primary particle size on the CAAM signal was investigated because of its likely relevance for biological effects, given that the particle size has a well-known and usually strong effect on the activity of a catalyst.

DEVICE DESCRIPTION AND METRIC

Operating Principle

The CAAM analyzes catalytic activity in two steps: At first, airborne particles containing the suspected catalyst material are sampled during a pre-determined time interval onto a glass fibre filter (Machery-Nagel, MN QF-10). The amount of material required is usually on the order of micrograms, as we shall see later on. After sampling is completed and without removing the filter from its housing, the accumulated particles are exposed to a flow of pre-mixed (and if necessary pre-heated) reaction gases to initiate a catalytic reaction. The choice of reaction gases is catalyst specific and pre-selected according to the type of active material anticipated in the aerosol. The concentrations of specific gases are measured by an appropriate sensor. This concentration signal is thus the primary measure for the airborne catalyst activity.

What is in fact measured by the CAAM?

The CAAM does not provide a direct measure for the mass (or number or surface area) of the catalyst aerosol sampled on the filter but for its activity. In the science and practice of catalyst design, it is well established that activity is not merely a function of catalyst mass but of various additional factors such as primary particle size (hence the specific surface area of the material) and the type of 'inert' support material in contact with the active phase. In the reality of workplace exposure measurements to potentially harmful aerosols, none of this additional information on catalyst structure is known *a priori*.

By expressing the amount of accumulated material directly via its catalytic activity, the CAAM in fact bypasses these complications and provides a

CAC, i.e. the activity per volume of sampled aerosol. This is a new metric for exposure assessment in workplace air.

One could of course weigh the amount of accumulated aerosol sampled by the CAAM to obtain gravimetric data as well. Unfortunately, workplace air is rarely made up of only one single species so that the catalyst mass may only represent a fraction of the total aerosol concentration present. To gain specific information about this fraction, expensive offline techniques such as optical or mass spectrometry are required. (A part of this study is dedicated to the investigation of the degree of interference of background aerosols with the CAAM signal.)

Despite the advantage of providing a more direct measure for activity, the current embodiment of the CAAM is based on a 'non-biological' chemistry. Nevertheless, the catalytic activity or surface reactivity of nanoparticles is considered a biological risk factor (Oberdoerster et al., 2005; Nel et al., 2006; Duffin et al., 2007) for which the CAAM can give a more direct indication than other aerosol measurement techniques.

Components of the CAAM

The laboratory prototype used consists of three main components described below in more detail (Fig. 1). Currently, all components are placed in a box with overall dimensions of $45 \times 30 \times 25\,cm^3$.

Sampling and Reaction Unit. This part of the detector is involved in both steps of the detection process; it first serves as an aerosol sampler by filtration and then as a reactor for the catalytic reaction. It consists of a custom-built filter housing which is connected to a small pump (SG10-2 from GSA). To avoid particle losses due to thermophoresis and a morphological change of the particles at elevated temperatures, the particles are sampled at room temperature, even if the chosen reaction requires elevated temperatures. When sampling is completed, the flow of ambient air is immediately switched over to a flow of reactant gases as described below. Thereby any handling or a contamination of the particles can be avoided.

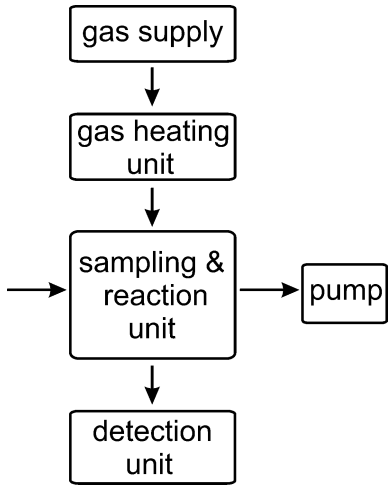

Fig. 1. Schematic of the CAAM functional components.

Gas Supply and Heating Unit. The required reactant gases are provided from small lecture bottles equipped with miniaturized pressure reducers. In addition, a space-saving gas flow control without the need of a power supply is integrated in the CAAM. A small heat exchanger, which is at this stage of development non-battery operated, is installed for the use of catalytic reactions which require pre-heated reaction gases. The heating unit is switched on after the sampling step in order to provide the educt gases at the required temperature which can be achieved within a few minutes (e.g. 2 min to reach a temperature of 450°C, which is required for the detection of nickel as we shall see later on).

Detection Unit. The concentration of specific gases and hereby the catalytic activity of the particles is measured by a non-dispersive IR sensor (smartMODULFLOW, smartGAS Mikrosensorik GmbH). Depending on the type of nanoparticles in the workplace and the chosen catalytic reaction, a suitable gas sensor has to be chosen, which allows the quantification of the appropriate product gases at concentrations of only a few ppm. The sensitivity of the IR sensor and the possibility of getting information on the gas composition in real time are important advantages of this method.

EXPERIMENTAL STRATEGY AND PROCEDURES

The laboratory prototype was investigated with regard to its activity response curve and its ability to detect catalytically active material against a background of inert aerosols. The measurements were performed with well-characterized aerosols produced continuously: catalytically active palladium and nickel nano-aerosols by a spark discharge technique; inert 'background' aerosols in

the submicron size range by decomposition of metal-organic precursors.

The response of the CAAM was measured for a range of catalyst aerosol mass concentrations and - in the case of palladium - also for several very accurately known primary particle sizes. These data were then used to estimate minimum sampling times required for a range of catalyst aerosol concentrations typically reported in the literature.

Generation and Characterization of Airborne Catalyst Particles

Nano-aerosols of either palladium or nickel were produced using a spark discharge generator built according to a well-known principle (Schwyn et al., 1988; Kruis et al., 1999). A spark discharge between two metallic electrodes (in this case palladium or nickel with a purity of 99.99%) provides the energy necessary to evaporate small amounts of metal, which immediately recondenses to form primary particles in the range of a few nanometers by homogeneous nucleation. These particles are swept from the discharge region by a constant flow of nitrogen (99.99%) at a rate of 1 l/min. Due to their high initial concentration, the primary particles form agglomerates before leaving the generator.

The production rate of the spark discharge generator, i.e. the mass concentration of the aerosols, was determined from filter samples by inductively coupled plasma optical emission spectroscopy (ICP-OES). The number concentration and agglomerate size distributions (i.e. the size distribution of the aerosols, Fig. 2) were measured by an electrical mobility spectrometer (SMPS, a combination of TSI DMA 3071A and CPC 3775). The aerosol mass concentration was varied

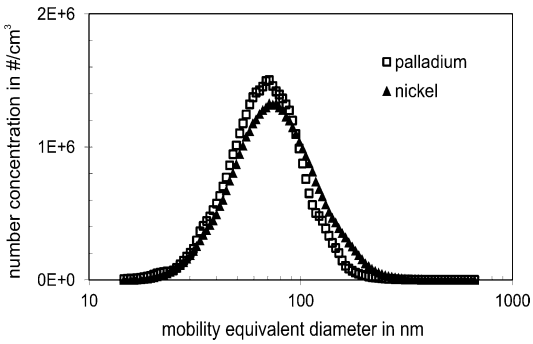

Fig. 2. Aerosol particle size distributions for palladium and nickel determined by SMPS.

Table 1. Characteristics of palladium and nickel aerosols directly after their production by spark discharge.

	Palladium	Nickel
Modal aerosol particle diameter (nm)	71	74
Number concentration (10^7 #/cm^3)	4.5	4.1
Mass concentration (mg/m^3)	16.7	6.5
Median primary particle size (nm)	3.2	3.5
BET surface area (m^2/g)	87	138

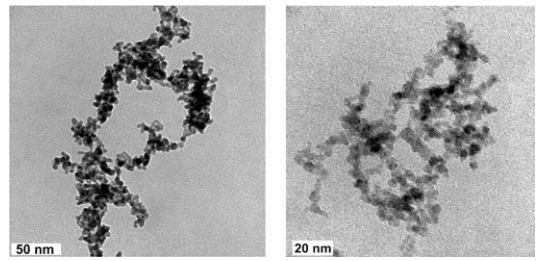

Fig. 3. TEM images of a palladium (left) and a nickel (right) agglomerate produced by spark discharge.

by dilution with 1, 2, or 3 l/min of additional N_2 to give mass concentrations of between about 3 and 16.7 mg/m^3. For details see Table 1.

The surface area of the agglomerates was identified by nitrogen BET (Quantachrome Nova 1200). Figure 3 shows typical transmission electron microscope (TEM) images of a palladium and a nickel agglomerate sampled directly at the exit of the generator. The geometric diameters of the primary particles were determined by TEM (Philips CM12, 120 kV). As expected, the primary particle sizes produced by the generator were fairly constant for the two aerosols. Larger palladium primary particles were generated by thermal conditioning of the aerosol in a tube furnace at temperatures up to 600°C. The overall range of primary particle diameters was between 3 and 30 nm.

Preparation and Characterization of Airborne Mixed Aerosols of Inert and Active Material

Ambient indoor aerosols are rather variable in composition with a broad size distribution which typically peaks somewhere between 0.1 and 1 µm. We therefore decided to generate surrogate background aerosols of silica, titania, or alumina in this range by chemical vapor synthesis (CVS). For this purpose, the respective metal alkoxides tetraethylorthosilicate (TEOS, $Si(OC_2H_5)_4$, purity of 99%), titanium tetraisopropoxide (TTIP,

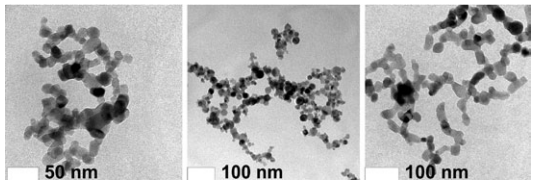

Fig. 4. TEM images of the oxidic background agglomerates silica, titania, and alumina (from left to right).

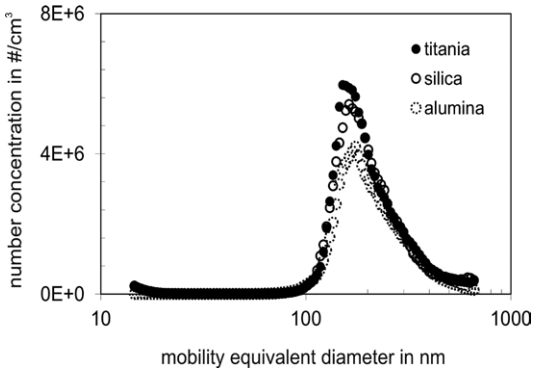

Fig. 5. Aerosol particle size distributions determined by SMPS for the three types of background aerosol.

$Ti(OC_3H_7)_4$, 97%), and aluminium-sec-butoxide ($C_{12}H_{27}O_3Al$, 98%), purchased from abcr, were used as precursors. They were evaporated into pure nitrogen (99.99%) at 60°C and then fed to a tube furnace where they decompose at 900°C and form particles by homogenous nucleation. These primary particles agglomerate further to aggregates in the range of several hundred nanometers.

The aerosols were characterized at the generator exit by TEM (Fig. 4) and SMPS (Fig. 5) using the same techniques as described previously for palladium and nickel. A summary of the properties of background aerosols is given in Table 2.

In order to generate internally mixed airborne particles consisting of both catalyst and background material, the two aerosols had to be mixed and coagulated. This was done by feeding them continuously through a 10-l mixing chamber at roughly equal number of concentrations and a combined flow rate 1.3 l/min. The setup and images of the resulting mixed particles are shown in Fig. 6.

Table 2. Characteristics of the background aerosols directly after their production by CVS.

	Silica	Titania	Alumina
Modal aerosol particle diameter (nm)	45	48	51
Number concentration (10^7 #/cm^3)	10.1	11.4	8.7
Median primary particle size (nm)	163	151	174

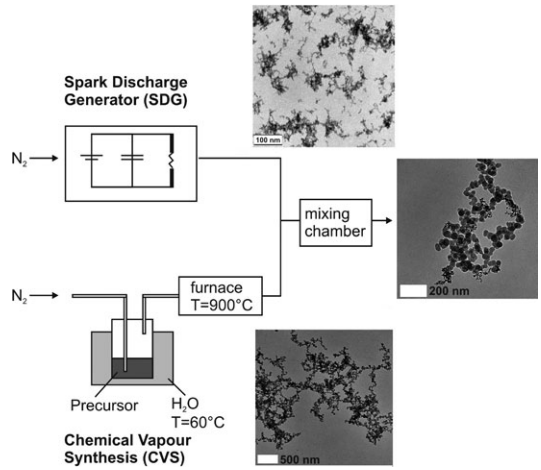

Fig. 6. Setup for the generation of mixed aerosol particles of catalyst and background agglomerates with typical TEM images of the particles before and after the mixing chamber.

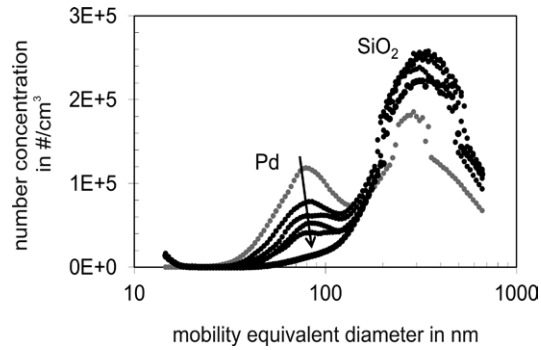

Fig. 7. Evolution of the particle size distribution in the mixing chamber in time steps of 2 min from start of chamber filling to steady state. The palladium peak at $t = 0$ min (grey curve) disappears within 10 min by attachment; the SiO_2 peak remains largely unchanged.

The mixing chamber was dimensioned to provide sufficient residence time for coagulation between the two aerosols to run to completion. This was verified, however, by a series of SMPS measurements of the aerosol size distribution at the chamber outlet. Figure 7 shows the evolution in time of the particle size distribution measured at 2-min intervals from the beginning of filling. With progressive filling, the right-hand peak consisting initially of pure silica particles quickly reaches a steady-state value. The left-hand peak corresponding to the palladium nano-agglomerates decreases monotonously during this time due to their

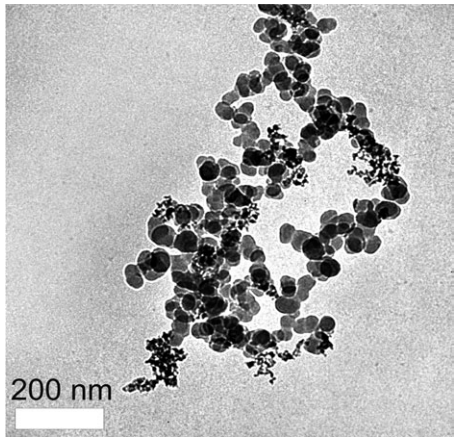

Fig. 8. TEM image of a mixed agglomerate of silica with attached palladium agglomerates (the finer component) sampled after 10 minutes of coagulation time.

attachment to the larger silica particles. Within 10 min, the unattached palladium aerosol has disappeared completely as a result of the coagulation process. The mixed state of the resulting particles is also visible from TEM images taken at the chamber outlet (Fig. 8). In conclusion, it is sufficient to wait for 10 min to achieve a complete attachment of the catalyst to the background particles.

Model Reactions for the Catalytic Activity

The detection of particles by their catalytic activity is based on catalytic reactions which are specific to the type of nanoparticle anticipated in the workplace air. The reactions chosen for this investigation are all well known and based on gaseous reactants and reaction products.

Detection of Palladium via the Hydrogenation of Ethene

The well-known hydrogenation reaction

$$C_2H_4 + H_2 \rightarrow C_2H_6$$

was selected because it produces a gaseous reaction product and runs at ambient temperature, thereby eliminating the need for pre-heated educt gases. Its usefulness for the detection of palladium nanoparticles was demonstrated previously in practice (Neubauer et al., 2011). For the purposes of this study, the reactant gases C_2H_4 and H_2 were pre-mixed in a lecture bottle containing 10 vol% of ethene (99.9%) and 10 vol% of hydrogen (99.9%), the balance being nitrogen (99.999%).

Incidentally, despite the fact that this is a well-known and frequently studied chemical reaction, there is some controversy in the literature with regard to structure sensitivity, i.e. the dependence of the activity on the size of the primary particles. In addition, there seems to be some influence of the support material on the catalytic reaction as well (Binder et al., 2009). These two factors were therefore taken into account when estimating the sensitivity of the CAAM.

Detection of Nickel via the Oxidation of CO

The catalytic oxidation of CO via the reaction

$$2CO + O_2 \rightarrow 2CO_2$$

is also well investigated due to its simplicity and its importance, e.g. in the research of fuel cells. Because the oxidative potential of nanoparticles is believed to be one of the key factors causing their toxicity (Ayres et al., 2008; Xia et al., 2008; Kovacic and Somanathan, 2010), we chose an oxidation reaction to characterize the activity of the nickel aerosol. The oxidation of CO is also described as being structure sensitive and this may influence the catalytic signal of the CAAM as in the case of palladium. Note, however, that the influence of primary particle size is not addressed in this paper because this parameter was not varied. The reactant gases were supplied from a lecture bottle containing 5 vol% CO (99.997%) and 5 vol% O_2 (99.995%) pre-mixed in nitrogen (99.999%) and pre-heated to 450°C before feeding them to the CAAM.

Data Evaluation

To provide a measure for the catalytic activity of palladium and nickel, the concentration of ethene or CO respectively was detected in the reactant gases (c_{in}) and in the gaseous reaction products (c_{out}). This was achieved by a quantification of these gases by the chosen IR sensors in intervals of 10 s. This allows the calculation of the conversion of ethene or CO, which served as a quantity for the expression of the catalytic activity of palladium and nickel. The conversion C was calculated according to the following equation:

$$C = \frac{c_{in} - c_{out}}{c_{in}}$$

The concentration c_{in} of ethene or CO was measured in parallel to the particle sampling step. To calculate the conversion, the mean of the last 10 measured concentration values prior to the initiation of the reaction was used. The concentration

c_{out} was determined 10 min after the start of the catalytic reaction as the catalytic signal needed some time to reach a steady state. Again, a mean of 10 concentration values was calculated for the determination of the conversion.

Typically, the conversion of a reaction is given in per cent or in arbitrary units (a.u.). We have chosen to use conversion expressed in arbitrary units as a measure for the catalytic activity of palladium and nickel aerosols. This activity was measured in dependence of the amount of particles sampled on the filter, which is at first the volume of the sampled aerosol. Because the mass concentrations of the nano-aerosols were very stable as verified by ICP-OES, the volume of the sampled aerosol can be converted readily to sampled particle mass. However, we propose the use of a CAC defined as activity per volume of sampled air as the activity of a catalyst is not merely a function of mass alone. The CAC can be easily derived from the slopes of the curves, which give the catalytic signal as a function of the sample volume, as we shall see later on in more detail. Therefore, the CAC is given in l^{-1}.

RESULTS AND DISCUSSION

Detection of Pure Palladium Aerosol based on its Catalytic Activity

The following two figures show the catalytic signal (i.e. the conversion of the educt ethene in arbitrary units) as a function of the amount of palladium sampled on the filter. In Fig. 9, this amount is expressed in terms of the 'volume of sampled aerosol' at four different mass concentrations. The palladium primary particle size is constant with a median of 3.2 nm. Each data point represents a minimum of three repetitive

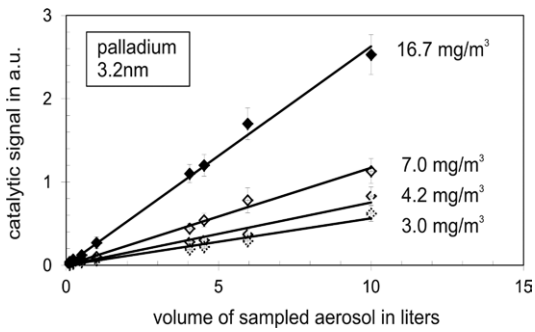

Fig. 9. CAAM signal versus volume of sampled palladium aerosol for different aerosol mass concentrations.

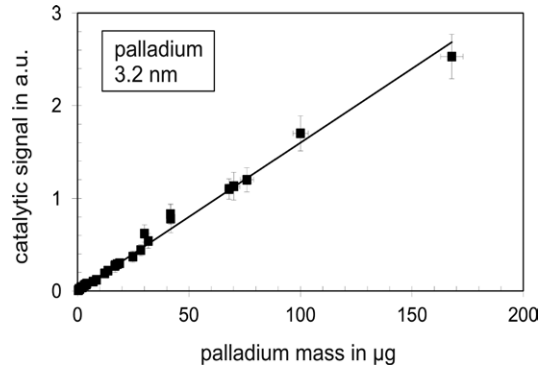

Fig. 10. CAAM signal versus sampled mass of the palladium aerosol.

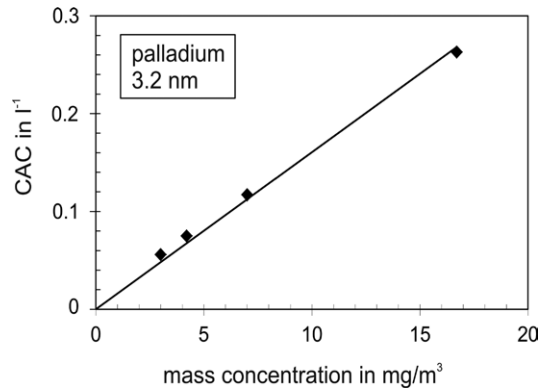

Fig. 11. Catalytic activity concentration versus mass concentration of the palladium aerosol.

measurements. Apparently the response curves are linear.

Because the mass concentration of the palladium aerosol generator was very stable, the volume of the sampled aerosol from Fig. 9 can be converted readily to 'sampled palladium mass' as shown in Fig. 10. Evidently, the CAAM response to catalyst mass (for a constant palladium primary particle diameter) is also linear within the accuracy of our measurements.

We now proceed from discussing the raw catalytic signal of the CAAM to its response in terms of a CAC, defined as the activity per volume of sampled aerosol. Given the linearity of the response curves, one can derive the CAC from the slope of any of the curves in Fig. 9. These values are plotted in Fig. 11 against the palladium mass concentration.

The linear relationship between CAC and mass concentration was expected for a fixed primary particle size. The dependence of the CAAM

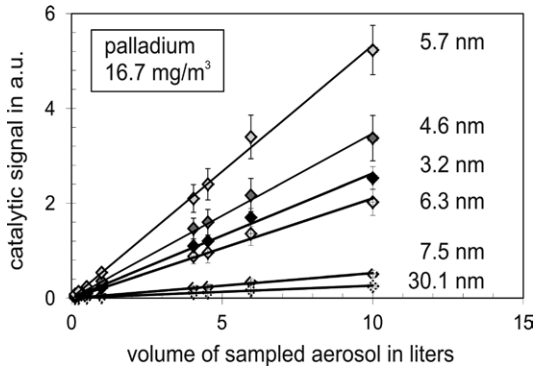

Fig. 12. CAAM signal versus volume of sampled palladium aerosol for different primary particle sizes.

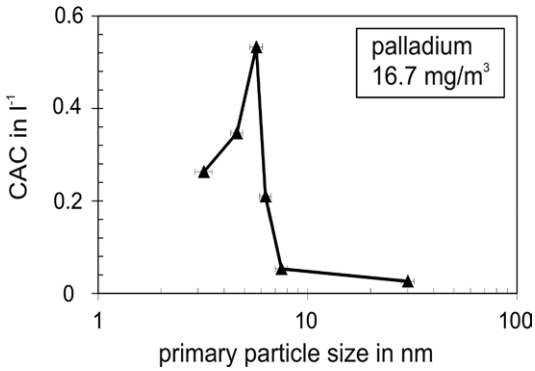

Fig. 13. Catalytic activity concentration versus primary particle size.

response to variations in the palladium primary particle diameter is discussed in the following. Figure 12 shows this dependence in terms of 'sampled aerosol volume', each data point representing a minimum of three measurements at a mass concentration of 16.7 mg/m^3. Obviously, a linear dependence is given again, whereas the differently sized palladium particles lead to diverging activity signals. With regard to device performance, this ability to resolve such differences is an indication of its sensitivity. More importantly, however, it confirms that catalyst mass alone - which could be measured by more conventional means such as offline chemical analysis of filter samples - is not a unique descriptor for the catalytic activity of aerosols and therefore not an adequate metric. The proposed concept of 'activity concentration', however, takes such effects into account.

CACs can again be derived from the slopes of the curves. They are shown in Fig. 13 as a function of the palladium primary particle size, with a very sharp maximum at 5.7 nm.

Detection of Pure Nickel Aerosol based on its Catalytic Activity

In analogy to the preceding results for palladium, Fig. 14 shows the catalytic signal for nickel as determined by the CAAM (i.e. the conversion of the educt CO in arbitrary units) as a function of the volume of the sampled nickel aerosol. Each data point again represents a minimum of three measurements. The experiments were performed at a constant setting of the nickel aerosol generator with regard to primary particle size. TEM analysis did not show any change in primary particle size due to exposure of the filter sample to pre-heated educt gases. This was somewhat surprising, given that earlier work (Seipenbusch et al., 2003; Weber et al., 2003) did show some sintering of nickel under comparable conditions. This aspect will be investigated in more detail in the future but has no bearing on the current conclusions.

As in the case of palladium, the CAAM response is reasonably well approximated by linear regression either for sample volume or for sampled aerosol mass (not shown here).

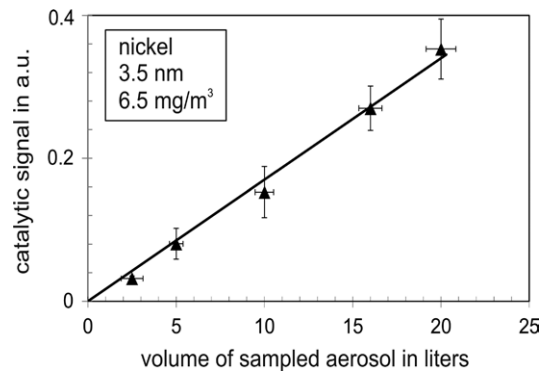

Fig. 14. CAAM signal versus volume of sampled nickel aerosol for a fixed primary particle size and aerosol concentration.

Detection of Palladium attached to Background Particles based on its Catalytic Activity

Figure 15 compares the CAAM response for pure palladium with that of palladium attached to various types of 'inert' particles. The aerosol mass concentration of palladium is constant at 16.7 mg/m^3. Measurements were made with two palladium primary particle sizes (3.2 and 5.7 nm). Each data point represents the mean of at least three measurements.

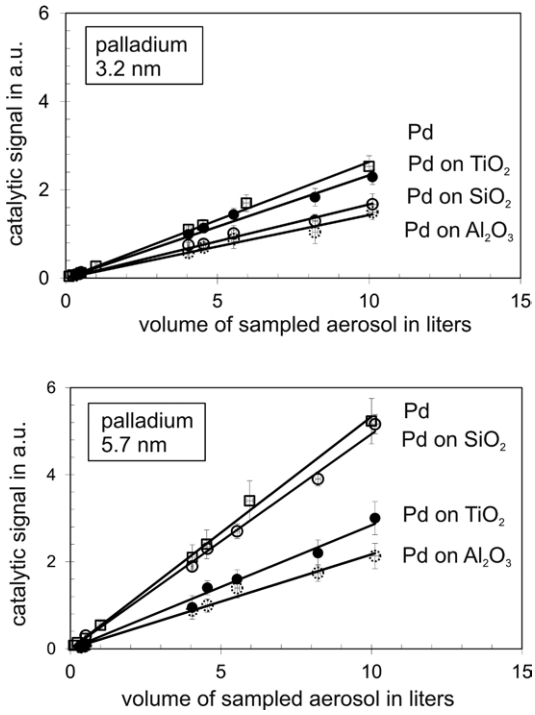

Fig. 15. CAAM signals for attached and unattached palladium nanoparticles as a function of sampled aerosol volume. The slopes represent CACs.

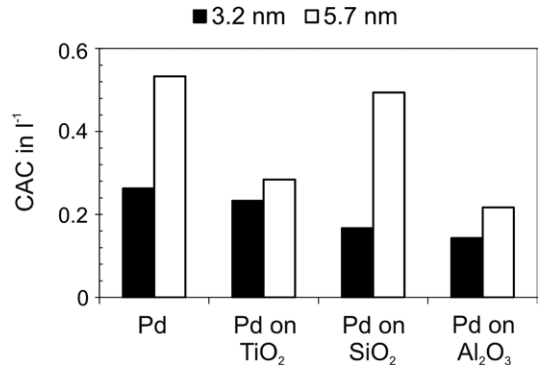

Fig. 16. Catalytic activity concentration of pure palladium particles with a primary particle size of 3.2 and 5.7 nm in comparison with palladium attached to silica, titania, and alumina.

We see that the CAAM response is proportional to the amount of sampled aerosol even when the palladium nanoparticles are attached to other material. The pure palladium particles always produce the strongest catalytic signal while the influence of the oxidic carrier materials depends somewhat on the palladium diameter. As purely oxidic background particles without any noble metal attached did not show a detectable activity with the CAAM, the catalytic signals shown in Fig. 15 are, therefore, most likely due to palladium, however, with an additional dependence on the type of background particles. These effects can also be seen in Fig. 16, which compares the catalytic activity concentrations derived from the slopes in Fig. 15 for the different combinations of materials.

From a catalysis point of view, such an influence of the carrier material was to be expected because oxidic support materials can interact with the active phase to modify the overall activity (Weber et al., 2006; Binder et al., 2009). When discussed from the perspective of this paper, however, these results demonstrate first of all that the CAAM is able to detect the active nanoparticles even when they are attached to background aerosols. Also the data lend further support to a point made previously that the catalytic activity of an aerosol is not simply proportional to accumulated mass but to other factors as well, which the CAAM inherently takes into account via the CAC. Catalytic activity concentration is, therefore, a more realistic metric for the detection of catalytically active aerosols.

CAAM Sensitivity and Required Sampling Times

CAAM sensitivity, i.e. the magnitude of the activity signal for a given amount of sampled catalyst, depends on the detection threshold of the IR detector built into the device. For an earlier embodiment of the device which was equipped with a full-scale laboratory FTIR as detector (Neubauer et al., 2011), the lower detection limit for reaction products was on the order of 10 p.p.m., resulting in extrapolated (theoretical) detection limits of 2 ng for palladium and about 2 µg for nickel and platinum respectively (disregarding for the moment any influence of primary particle size etc.). The lower detection thresholds for the current prototype have not been exactly determined yet. However, for the measurements reported here, the smallest detected masses were about 2 µg for palladium and 16 µg for nickel. Using these values, one can express the sensitivity of the CAAM in terms of sampling time required to accumulate these amounts of catalyst on the filter.

The maximum sampling flow rate of the CAAM is 10 l/min, determined by the personal sampling pump in current use in the CAAM. Typical catalyst mass concentrations in workplace air can be found in the literature. Reports for palladium are in a range of 1 µg/m^3 to 1 mg/m^3 (Kielhorn et al., 2002; World Health Organization, 2002)

Table 3. Required sampling times for an accumulated mass of 2 µg of palladium, assuming a sample flow rate of 10 l/min and a workplace mass concentration in the range between 1 µg/m^3 and 1 mg/m^3.

Palladium concentration in workplace air (mg/m^3)	Sampling time for 2 µg Palladium (min)
1	<1
0.1	<2
0.01	19
0.001	190

Table 4. Required sampling times for an accumulated mass of 16 µg of nickel, assuming a sample flow rate of 10 l/min and a mass workplace concentration in the range between 10 µg/m^3 and 10 mg/m^3.

Nickel concentration at workplace (mg/m^3)	Sampling time for 16 µg Nickel (min)
10	<1
1	<2
0.1	16
0.01	160

for metallic nickel in the range of 10 µg/m^3 to 10 mg/m^3 (Nickel Institute, 2008).

The range of sampling times calculated on the basis of these values is summarized in Tables 3 and 4. On the high end of the expected particle concentrations, we see that the required mass of either metal can be accumulated within a few minutes, whereas in the mid-range of concentration still only about 20 min are required (please note that after the particle sampling, it takes only 10 min more to get the catalytic signal). Obviously, the sampling times could be further reduced by increasing the sampling rate or other practical measures. For these reasons, one can consider the CAAM a quasi real-time detector, compared with offline techniques such as ICP-OES or ICP-MS, which are on the one hand much more sensitive but on the other hand require considerably more time for sample preparation and analysis. As the currently proposed exposure limits for nickel (OSHA: 1 mg/m^3, NIOSH: 0.015 mg/m^3) (to our knowledge, currently no exposure limits for palladium are defined) are in the same range as the mass concentrations on which we based our calculations, the evaluated sampling times of the CAAM underline its usefulness in the assessment of workplace air in quasi real-time.

CONCLUSIONS

A new type of detector for exposure assessment to catalyst nanomaterials in workplace air has been presented. The response of this detector was investigated towards its capability for a substance-specific detection of such nanoparticles based on their catalytic activity, regardless of the presence of a background aerosol.

Using a portable laboratory prototype, the device response was successfully characterized for catalytically active palladium and nickel nano-aerosols. Measurements were also made with the catalyst particles attached to larger aerosol particles of titania, silica, and alumina, in order to simulate the presence of natural background aerosols.

A few micrograms of sampled material were found to be sufficient for reliable detection of the catalysts, also in the presence of background aerosols, leading to an analysis time on the order of minutes. This makes the CAAM a substance-specific quasi real-time detector for (known) airborne catalysts, also when they were attached to background particles.

The CAAM expresses the presence of the catalyst directly in terms of a catalytic activity concentration, rather than its mass concentration, which is shown not to be a unique descriptor for its activity. This is a new metric to express the presence of a catalyst material in terms of its functionality, thereby bypassing the ongoing discussion about the appropriateness of other metrics such as number, surface area, or mass concentration. The activity concentration accounts inherently for changes in catalytic activity of an aerosol due to age, agglomeration, or other factors.

In spite of these advantages, the concept in its current state also has limitations. For one, the CAAM uses one specific chemical reaction to express activity, whereas the effectiveness of a catalyst will of course vary with the type of reaction. Moreover, the detection principle of the CAAM is based on a 'non-biological' chemistry. Bridging the chain of evidence between non-biological and biological catalytic activities remains a project for the future.

FUNDING

European Commission (211464-2); smartGAS Mikrosensorik GmbH.

Acknowledgements—We gratefully thank the European Commission for the funding of the research leading to these results under grant agreement no 211464-2 (NANODEVICE) in the Seventh Framework Programme (FP7/2007–2013). We also gratefully acknowledge the support of Michael Maier from smartGAS Mikrosensorik GmbH.

REFERENCES

Ayres JG, Borm P, Cassee FR *et al.* (2008) Evaluating the toxicity of airborne particulate matter and nanoparticles by measuring oxidative stress potential–a workshop report and consensus statement. Inhal Toxicol; 20: 75–99.

Baron PA, Willeke K. (2001) Aerosol measurement. Principles, techniques and applications. New York: Wiley-Interscience.

Bergamaschi E. (2009) Occupational exposure to nanomaterials: present knowledge and future development. Nanotoxicology; 3: 194–201.

Binder A, Seipenbusch M, Muhler M *et al.* (2009) Kinetics and particle size effects in ethene hydrogenation over supported palladium catalysts at atmospheric pressure. J Catal; 268; 150–5.

Brouwer D. (2010) Exposure to manufactured nanoparticles in different workplaces. Toxicology; 269: 120–7.

Brouwer D, van Duuren-Stuurman B, Berges M *et al.* (2009) From workplace air measurement results toward estimates of exposure? Development of a strategy to assess exposure to manufactured nano-objects. J Nanopart Res; 11: 1867–81.

Duffin R, Tran L, Brown D *et al.* (2007) Proinflammogenic effects of low-toxicity and metal nanoparticles in vivo and in vitro: highlighting the role of particle surface area and surface reactivity. Inhal Toxicol; 19: 849–56.

Hester RE, Harrison RM. (2007) Occupational exposure to nanoparticles and nanotubes. In Mark D, editor. Nanotechnology: consequences for human health and the environment. Royal Society of Chemistry.

Kielhorn J, Melber C, Keller D *et al.* (2002) Palladium–a review of exposure and effects to human health. Int J Hyg Environ Health; 205: 417–32.

Kovacic P, Somanathan R. (2010) Biomechanisms of nanoparticles (toxicants, antioxidants and therapeutics): electron transfer and reactive oxygen species. J Nanosci Nanotechnol; 10: 7919–30.

Kruis FE, Fissan H, Peled A. (1999) Synthesis of nanoparticles in the gas phase for electronic, optical and magnetic applications—a review. J Aerosol Sci; 29: 511–35

Kuhlbusch TA, Asbach C, Fissan H*et al.* (2011) Nanoparticle exposure at nanotechnology workplaces: a review. Part Fibre Toxicol; 8: 22. doi:10.1186/1743-8977-8-22

Kuhlbusch TAJ, Fissan H, Asbach C. (2009) Nanotechnologies and environmental risks—measurement technologies and strategies. In Linkov I and Steevens J, editors. Nanomaterials: risks and benefits. Dordrecht, The Netherlands: Springer, pp. 233–43.

Maynard AD, Aitken RJ. (2007) Assessing exposure to airborne nanomaterials: current abilities and future requirements. Nanotoxicology; 1: 26–41.

Methner M, Hodson L, Dames A *et al.* (2009) Nanoparticle emission assessment technique (NEAT) for the identification and measurement of potential inhalation exposure to engineered nanomaterials—part B: results from 12 field studies. J Occup Environ Hyg; 7: 163–76. doi:10.1080/15459620903508066

Murashov V, Engel S, Savolainen K *et al.* (2009) Occupational safety and health in nanotechnology and organisation for economic cooperation and development. J Nanopart Res; 11: 1587–91.

Nel A, Xia T, Mädler L *et al.* (2006) Toxic potential of materials at the nanolevel. Science; 311: 622–7.

Neubauer N, Weis F, Binder A *et al.* (2011) A highly sensitive technique for detecting catalytically active nanoparticles against a background of general workplace aerosols. J Phys: Conf Ser; 304. doi:10.1088/1742–6596/304/1/012011

Nickel Institute. (2008) Safe use of nickel in the workplace—a guide for health maintenance of workers exposed to nickel, its compounds and alloys. Third edition. http://nickelinstitute.org/en/MediaCentre/Publications/~/media/Files/MediaCentrePublications/HG%203rd%20Ed%202008.ashx#Page=1

Oberdörster G, Maynard A, Donaldson K *et al.*; ILSI Research Foundation/Risk Science Institute Nanomaterial Toxicity Screening Working Group. (2005) Principles for characterizing the potential human health effects from exposure to nanomaterials: elements of a screening strategy. Part Fibre Toxicol; 2: 8.

Peters TM, Elzey S, Johnson R *et al.* (2008) Airborne monitoring to distinguish engineered nanomaterials from incidental particles for environmental health and safety. J Occup Health Environ Hyg; 6: 73–81. doi:10.1080/15459620802590058

Savolainen K, Alenius H, Norppa H *et al.*. (2010a) Risk assessment of engineered nanomaterials and nanotechnologies–a review. Toxicology; 269: 92–104.

Savolainen K, Pylkkänen L, Norppa H *et al.*. (2010b) Nanotechnologies, engineered nanomaterials and occupational health and safety—a review. Safety Sci; 48: 957–63.

Schwyn S, Garwin E, Schmidt-Ott A. (1988) Aerosol generation by spark discharge. J Aerosol Sci; 19: 639–42.

Seipenbusch M, Binder A, Kasper G. (2008) Temporal evolution of nanoparticle aerosols in workplace exposure. Ann Occup Hyg; 52: 707–16.

Seipenbusch M, Weber AP, Schiel A *et al.* (2003) Influence of the gas atmosphere on restructuring and sintering kinetics of nickel and platinum aerosol nanoparticle agglomerates. J Aerosol Sci; 34: 1699–1709.

Tsai SJ, Ada E, Isaacs J *et al.* (2009) Airborne nanoparticle exposures associated with the manual handling of nanoalumina and nanosilver in fume hoods. J Nanopart Res; 11: 147–61.

Weber AP, Davoodi P, Seipenbusch M*et al.* (2006) Catalytic behaviour of nickel nanoparticles: gasborne vs. supported state. J Nanopart Res; 8: 445–53.

Weber AP, Seipenbusch M, Kasper G. (2003) Size effects in the catalytic activity of unsupported metallic nanoparticles. J Nanopart Res; 5: 293–98.

Weber AP, Davoodi P, Seipenbusch M *et al.* (2006) Catalytic behaviour of nickel nanoparticles: gasborne vs. supported state. J Nanopart Res; 8: 445–53.

World Health Organization. (2002) Environmental Health Criteria 226—Palladium.

Xia T, Kovochich M, Liong M *et al.* (2008) Comparsion of the mechanism of toxicity of zinc oxide and cerium oxide nanoparticles based on dissolution and oxidative stress properties. ACS Nano; 2: 2121–34.